Microsyst Technol
DOI 10.1007/s00542-015-2429-3

TECHNICAL PAPER

Electromechanical modeling and simulation by the Euler–Lagrange method of a MEMS inertial sensor using a FGMOS as a transducer

G. Stephany Abarca-Jiménez · M. Alfredo Reyes-Barranca · Salvador Mendoza-Acevedo · Jacobo E. Munguía-Cervantes · Miguel A. Alemán-Arce

Received: 7 January 2015 / Accepted: 13 January 2015

Abstract In this paper, the electromechanical modeling of a differential capacitive sensor interconnected with a floating-gate MOS (FGMOS) transistor is shown; the model was obtained using the Euler–Lagrange theory to analyze this particular physical system used as an inertial sensor. A design methodology is also shown relating all the physical parameters involved, such as: stiffness, damping associated with the capacitive structure, parasitic capacitances present in the transistor, and the maximum operating voltages to avoid pull-in effect. Cases for symmetric and non symmetric differential capacitance comb arrays are analyzed. A model comparison between conventional mass–spring–damper mechanical systems to a specific electromechanical system for capacitive sensor with its associated readout electronics is shown.

G. S. Abarca-Jiménez (✉) · M. A. Reyes-Barranca
Department of Electrical Engineering, CINVESTAV IPN, 07360 Mexico City, Mexico
e-mail: gabarca@cinvestav.mx

M. A. Reyes-Barranca
e-mail: mreyes@cinvestav.mx

S. Mendoza-Acevedo
Centro de Investigación en Computación-Instituto Politécnico Nacional, 07738 Mexico City, Mexico
e-mail: smendoza@cic.ipn.mx

J. E. Munguía-Cervantes · M. A. Alemán-Arce
Centro de Nanociencias y Micro y Nano Tecnologías-Instituto Politécnico Nacional, 07738 Mexico City, Mexico
e-mail: jmunguia@ipn.mx

M. A. Alemán-Arce
e-mail: maleman@ipn.mx

1 Introduction

Mathematical modeling of systems along the time has been an extremely useful tool in many areas of science and technology. System modeling is a procedure that allows description, by means of physical laws, of the dynamics of a given system. When a model is established it is important to keep balance between simplicity and accuracy; however, it should be considered that as the more accurate the model is, the greater its complexity will be. The importance of building up a good model relies on the ability to distinguish between variables of high importance describing the system and those variables that are irrelevant for determining the state of the system. Building a good model greatly facilitates the understanding of the physics of the system and also allows predicting the performance under practical conditions. Mathematical modeling systems are widely used in areas such as control systems as is the case of Zhang and Liu (2007) where a classical Euler–Lagrange model was proposed for establishing a novel algorithm for gain control. Another good example using the classical theory of Euler–Lagrange equation was reported in Zeng et al. (2011) in which a novel approach is presented for modeling an inclined drum washing machine system. Other examples of novel mathematical models that describe dynamic systems using the theory of Euler–Lagrange as well are shown in Croci et al. (2012). This theory is a useful mathematical tool when it comes to describe the dynamics of electromechanical system; when you want to describe the dynamics of a CMOS–MEMS device, it becomes particularly useful given the high level of integration of mechanical sensors or actuators together with signal processing and control electronics usually present in modern systems.

There are other ways to model MEMS sensors as shown in Su and Chong (2005), where an automatic process is

Published online: 01 February 2015

presented to generate the mesh of a MEMS model by using a geometric transformation, known as the block Cartesian abstraction. Another example is shown in Zhao et al. (2007). It presents a novel MEMS accelerometer model implemented in VHDL-AMS. In Pustan et al. (2010), it is described the studies of the mechanical characteristics of flexible MEMS based on finite element analysis (FEM) and experimental investigations. In Mezghani et al. (2013), a sensitivity behavior study and optimization of a dual axis CMOS–MEMS convective accelerometers is presented, using both analytical and FEM techniques. Nevertheless, all of the above papers are characterized because they model MEMS either mechanically or electrically, as separate models. In this paper, modeling and simulation of CMOS–MEMS capacitive structures used to sense acceleration is presented, showing a novel way to apply the classical theory of Euler–Lagrange modeling. In this model, a coupling between the mechanical and electrical elements included in the system is developed. The main advantage of this kind of model is that highly specialized finite element software is not required to simulate the behavior of the MEMS.

Based on the paper shown in Zeng et al. (2003), here it is proposed an innovative and general mathematical modeling framework with Lagrangian functions of multi-coupled energy domains for MEMS structures; hence, in this paper an electromechanical model for sensing accelerometers is proposed, where differential capacitance is used for symmetric or asymmetric comb drive design cases, applying this methodology to a capacitive transducer.

2 Structure of a capacitive sensor coupled with a FGMOS

The principle of differential capacitance transduction is widely used in the design of sensors given its advantages compared with other transduction principles based on piezoelectric or piezoresistive elements. The key benefit from the principle of differential capacitance highlights issues as its low dependence on temperature changes, its compatibility to be made in a standard CMOS process and easy miniaturization.

A differential capacitive transducer can be described by three basic parts: two fixed electrodes and a movable electrode. The movable electrode's task is to transduce force, either inertial or some other type of energy, deriving in a shift of an electrode; such movement will cause a change in capacitance between the movable electrode and the two fixed electrodes. Note that the capacitance will increase when the movable electrode approaches to the first fixed electrode, while the capacitance between the second fixed electrode and the movable electrode will decrease. In Fig. 1a the differential capacitance configuration is shown for the case of an accelerometer and in Fig. 1b the same configuration is shown for the case of a typical pressure sensor.

The dielectric usually used in this type of structure is air or silicon dioxide; for the case of structural layers it is common to use monocrystalline silicon, polysilicon or metal layers such as aluminum. Examples of such structures can be found in Van Toan and Ono (2014).

Consider now that the capacitive sensor is monolithically integrated including readout circuitry, with a floating-gate MOS transistor (FGMOS) as part of it. The equivalent circuit model is shown in Fig. 2a and the electromechanical model is shown in Fig. 2b.

The spring-mass system in Fig. 2b represents the movable part of the sensor, capacitors C_{11} and C_{22} represent capacitors formed between the movable electrode and fixed electrodes, V_C represents the voltage source connected to the control gate, while V_{DS} represents the voltage between the drain and the source of the FGMOS. In this case, the source is connected to ground; C_D represents the parasitic transistor capacitance between the overlap of gate and drain and C_{ox} is the channel capacitance, the rest of the parasitic capacitances are not considered in the analysis since the voltage at source and substrate is zero. Distances d_1 and d_2 represent the separation of the electrodes in rest (d_1 and d_2 can be symmetric or asymmetric). For the case in which both distances are symmetric, the system is represented by a single distance d, Fig. 3.

3 Mathematical model of the sensor

In this section, following Lagrange's theory a particular mathematical model for the capacitive sensor based on the calculation of the kinetic and potential energy of the system is presented. The main advantage of this type of modeling is that it is not required to apply neither Newton's nor Kirchhoff laws for modeling physical systems, something that may be rather cumbersome. As is the intention to demonstrate, this procedure is greatly advantageous when modeling monolithically integrated readout electronics together with MEMS, as system complexity increases every day, since the added feature comes out when a mechanical element (a spring, for example) used within the structure is at the same time a resistor or a capacitor forming part of an electrical circuit.

Although the Euler–Lagrange theory for systems modeling is a widely and well-known used basis, regarding MEMS sensors with integrated electronics it is interesting to adapt the equivalent model in consideration with actual physical elements, since the level of integration of the electrical–mechanical model can be high (as is the case presented here) due to the function duality of the system components, i.e., mechanical and electrical.

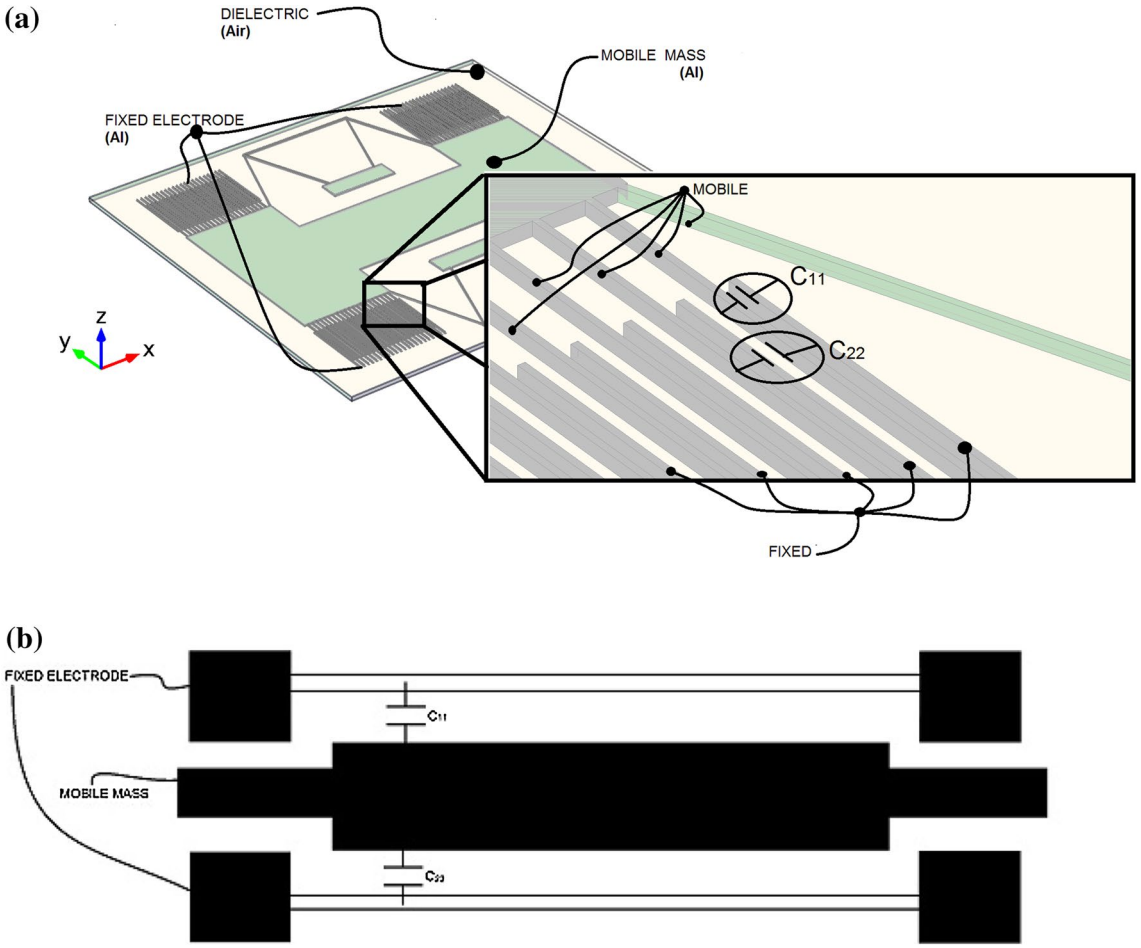

Fig. 1 Capacitive structures used in CMOS–MEMS, **a** isometric view of a typical accelerometer and **b** section view of a typical pressure sensor

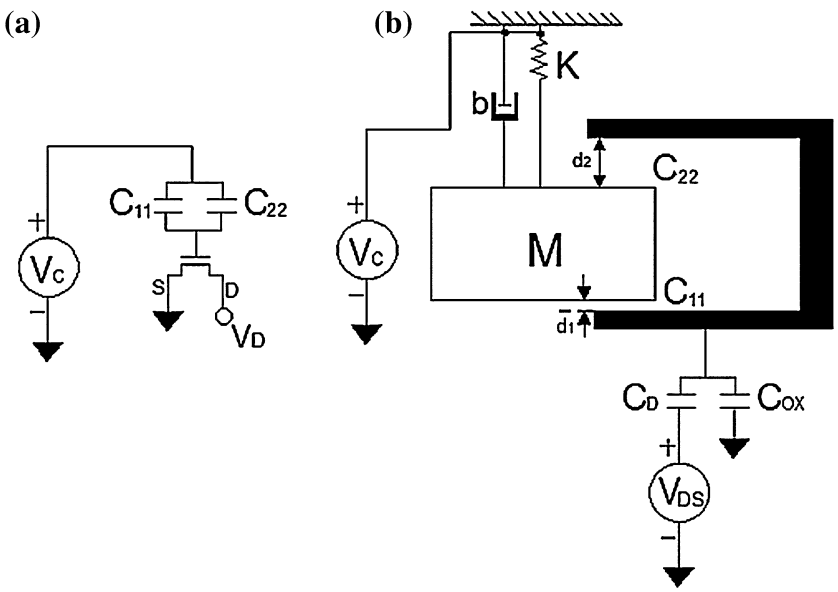

Fig. 2 Equivalent model, **a** electrical and **b** electromechanical

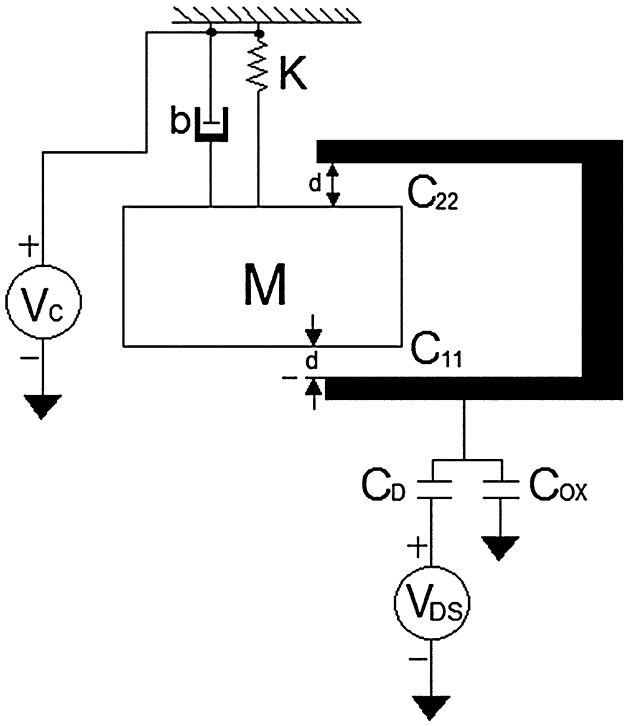

Fig. 3 Electromechanical model with a symmetric separation of d; when a force is applied C_{11} increases while C_{12} decreases

First, let's consider that the generalized coordinates (q_i) of the system are the set of independent variables to completely describe the present status. In this case, the circuit charges (q_1, q_2) and the displacement of the moving mass (x) will be the independent variables.

The Lagrangian (1) of the system is defined by the difference between kinetic and potential energy; in this case the element that adds kinetic energy to the system will be the moving mass, whereas the potential energy contribution involves several elements such as the spring that holds the movable mass, the comb drive capacitors and the parasitic capacitors of the FGMOS transistor. Finally, the power dissipation (2) will be given by the energy-dissipating element, which damps the movement of the moving mass.

$$L = \frac{1}{2}M\dot{x}^2 - \frac{1}{2}kx^2 - \frac{1}{2}\left[\frac{d_1d_2 - x(d_1 - d_2) - x^2}{A\varepsilon_0\varepsilon_r[d_1 + d_2]}\right] q_1^2 - \frac{1}{2}\left[\frac{1}{C_D}\right](q_1 - q_2)^2 - \frac{1}{2}\left[\frac{1}{C_{OX}}\right]q_2^2 \quad (1)$$

where L is the Lagrangian of the system; M is the movable mass; x is the displacement of the movable mass and the *first generalized coordinate*; k is the equivalent stiffness ratio of the system; b is the damping coefficient; d_1 and d_2 are the distance between electrodes in the static state; A is the overlap area between fingers of the comb drive; ε_0 permittivity of vacuum; ε_r relative permittivity of the medium; q_1 is the charge of the current mesh formed between the electromechanical system and the ground reference; C_D is the parasitic capacitance formed by the overlap of drain with the floating gate; q_2 is the charge of the current mesh formed between the shared node of C_{OX} with C_D and the ground reference; C_{OX} is the capacitance between channel and the floating gate.

$$D = \frac{1}{2}b\dot{x}^2 \quad (2)$$

Lagrange's equation for non-conservative systems with input forces is expressed in (3), where the input forces are known as generalized forces (Q_i), corresponding to the *i-th* generalized coordinate.

$$\frac{d}{dt}\left(\frac{\partial L}{\partial \dot{q}_i}\right) - \frac{\partial L}{\partial q_i} + \frac{\partial D}{\partial \dot{q}_i} = Q_i \quad (i = 1, 2, \ldots, n) \quad (3)$$

In this case, it was considered three generalized forces: the drain voltage, V_{DS}, the source voltage in the control gate, V_c, and the force due to applied acceleration in the movable mass, $f(t)$, which can be calculated by the Newton's second law.

For the case in which d_1 and d_2 are asymmetric, equations describing the dynamics of the system can be written as follows:

$$M\ddot{x} + b\dot{x} + kx - \left(\frac{q_1^2}{2A\varepsilon_0\varepsilon_r[d_1 + d_2]}\right)(2x + d_2 - d_1) = f(t) \quad (4)$$

$$\left(\frac{d_1d_2 - x(d_2 - d_1) - x^2}{A\varepsilon_0\varepsilon_r[d_1 + d_2]}\right)q_1 + \left[\frac{1}{C_D}\right](q_1 - q_2) = V_{DS} + V_c \quad (5)$$

$$\left[\frac{1}{C_{OX}}\right]q_2 - \left[\frac{1}{C_D}\right](q_1 - q_2) = V_{DS} \quad (6)$$

Otherwise, for a symmetric case, substituting d_1 and d_2 by d the later Eqs. (4), (5) and (6) are simplified as:

$$M\ddot{x} + b\dot{x} + kx - \left(\frac{q_1^2}{2A\varepsilon_0\varepsilon_r d}\right)(x) = f(t) \quad (7)$$

$$\left(\frac{d^2 - x^2}{2A\varepsilon_0\varepsilon_r d}\right)q_1 + \left[\frac{1}{C_D}\right](q_1 - q_2) = V_{DS} + V_c \quad (8)$$

$$\left[\frac{1}{C_{OX}}\right]q_2 - \left[\frac{1}{C_D}\right](q_1 - q_2) = V_{DS} \quad (9)$$

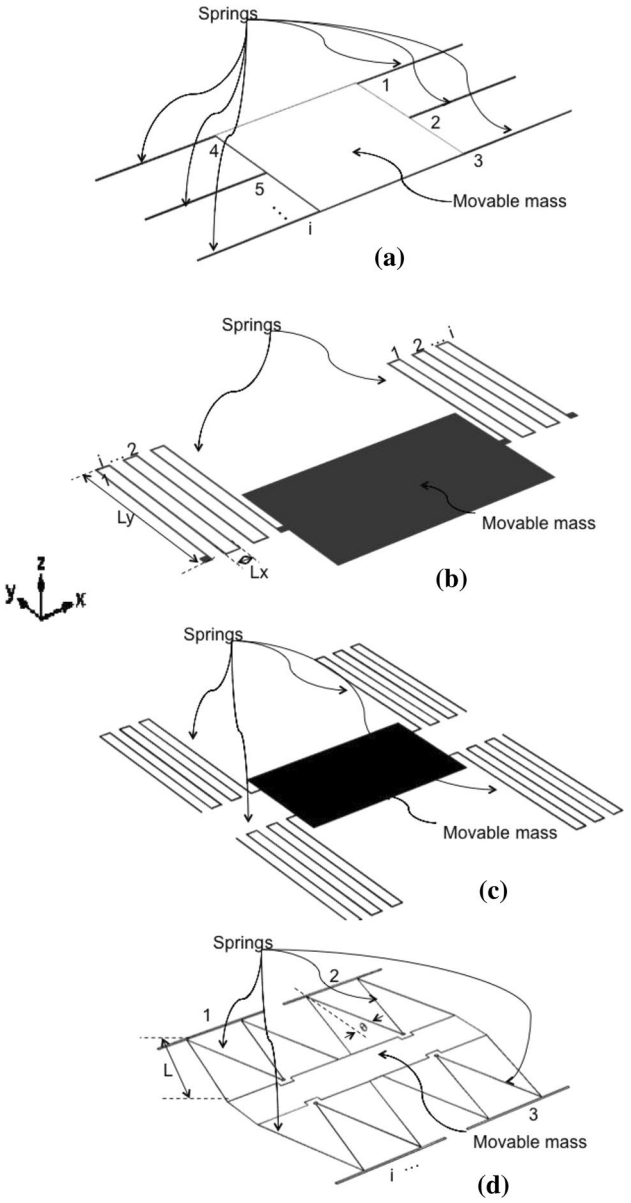

Fig. 4 Possible configurations for capacitive mobile structure

4 Determination of the parameters for the proposed mathematical model

In order to determinate the parameters of the model, it is necessary to first establish the value for some variables, like the proof mass and the acceleration range of the sensor. In this case, the value of the proof mass weight will be arbitrarily proposed to consider it as a known parameter, and the acceleration range of the sensor will be ±6G, since this range is commonly found in some commercial accelerometers; however this model is valid for different acceleration values also. In order to simulate the sensor with the model obtained in the previous section, initially, it will be necessary to calculate two mechanical parameters, being (1) the stiffness coefficient on the axis of interest, and (2) the damping factor associated to this stiffness coefficient, together with two electrical parameters like (1) the parasitic capacitances associated to the FGMOS and (2) the pull-in voltage of the capacitive sensor, either for comb drive or parallel plates designs.

4.1 Stiffness coefficient

The stiffness coefficient can be calculated with (10):

$$k_x = \frac{F}{x} \tag{10}$$

where F is the force applied to the structure due to acceleration or pressure, which can be calculated with the Newton's second law considering an acceleration of 9.81 m/s^2 (1G), and x is the desired displacement due to applied force. Furthermore, for the considered case and based on the electrostatics theory of the pull-in voltage of parallel plate capacitors, the maximum displacement allowed for the moving electrode must be:

$$x < \frac{1}{3}d \tag{11}$$

Now, in order to calculate the geometry of the structure that matches with the stiffness coefficient calculated before, consider the structures shown in Fig. 4. It is clear that for each structure, the stiffness coefficient will have different behaviors. The spring array on each side of all the presented structures is a parallel array of beams, because it is referred to the same mass and the same anchored part. The spring constant for the design will be exactly one half of the total spring constant.

For design A, the length for each beam will be:

$$L = \sqrt[3]{\frac{12EI}{\frac{1}{i}K_x}} \tag{12}$$

where E, is the Young's Modulus; I is the inertia moment; L is the length of the beam and i is the number of beams. The inertia moment for beams having a rectangular cross-section and movement along the x axis, as is the present case, can be calculated by:

$$I = \frac{tw^3}{12} \tag{13}$$

where t is the beam's thickness and w is the beam's width.

Next, for design B, it is preferable to calculate the value for Ly for a given value of Lx (see Fig. 4b) since the movement is along the x axis, and the beam Ly clearly governs the movement in that axis; for each beam with a length Ly, the expression will be:

$$\frac{2iK_x}{Et}L_y^4 + \frac{4iK_xL_x\left(\frac{w_y}{w_x}\right)^3}{Et}L_y^3 - 2w_y^3L_y - w_y^3L_x\left(\frac{w_y}{w_x}\right)^3 = 0 \tag{14}$$

where L_y and L_x are the beam's length, and w_y and w_x are the beam's width, along the y and x axes, respectively; i is the number of U-shaped beams on each side (see Fig. 4b).

Since it is desired to fabricate the structures with a CMOS technology, layers thickness is determined by the particular process, besides the mechanical design parameters are linked to these dimensions; in order to get a good performance, the width and thickness of each beam have to be related as follows:

$$2w_y < t \tag{15}$$

Furthermore, design C in Fig. 4c is an alternative of design B, where the length of the beam can be calculate by:

$$\frac{IK_x}{Et}L_y^4 + \frac{2iK_xL_x\left(\frac{w_y}{w_x}\right)^3}{Et}L_y^3 - 2w_y^3L_y - w_y^3L_x\left(\frac{w_y}{w_x}\right)^3 = 0 \tag{16}$$

Finally, for design D in Fig. 4d, the length of the beam can be calculated by:

$$L = \sqrt[3]{\frac{12EI\cos\theta}{\frac{1}{i}K_x}\left(1 + \frac{\cos\theta}{2}\right)} \tag{17}$$

where θ is the beam's angle and i is the number of triangular pairs.

4.2 Damping factor

Damping is the collection of all energy dissipating mechanisms in a structure; this phenomenon is associated with friction of a layer either against a solid or a fluid. In a mechanical structure three different types of damping can be identified: (1) damping due to a surrounding fluid, called viscous damping; (2) damping due to internal friction in the material, called elastic hysteresis; and (3) damping due to friction in the connection between structural members, called Coulomb friction (Huei-Huang 2012). In this case, the coulomb damping can be ignored, because due to the manufacturing process the sensor is composed of a single layer, and therefore there are no mechanical joints. In order to obtain the damping factor due to viscous damping and elastic hysteresis, we assume the coefficient b is a linear combination of the mass, m and the stiffness coefficient, k_x, this is (Huei-Huang 2012):

$$b = \alpha m + \beta k_x \tag{18}$$

where α and β are parameters used to characterize the damping property of a material. Using $b = 2\,m\xi\omega$ and $k = m\omega^2$, where ξ is the damping ratio and ω is the natural frequency of the structure, (18) can be written as follows:

$$2\xi\omega = \alpha + \beta\omega^2 \tag{19}$$

For many finite element software, as in the case of ANSYS® Workbench™ 14, a zero value for α is assumed, allowing β to be set as an input parameter for a time-dependent analysis. Besides, the damping ratio for typical structures ranges from 0.02 to 0.07 (Huei-Huang 2012).

$$b = \frac{2\xi}{\omega}k_x \tag{20}$$

Thus, it can be said that the damping parameter is a function of size of the moving mass and stiffness coefficient associated with the spring holding the movable mass.

4.3 Electrical parameters

4.3.1 Parasitic capacitance

C_{OX} and C_D are the parasitic capacitances associated with the model, due to the configuration in which the circuit is connected. Taking technological data from the selected CMOS process and proposing the aspect ratio of the FGMOS, it is possible to determine the value of the capacitors using (20) and (21):

$$C_D = \frac{\varepsilon_0\varepsilon_{ox}WL_D}{t_{ox}} \tag{20}$$

$$C_{ox} = C'_{ox}WL \tag{21}$$

where ε_0 is the permittivity of vacuum; ε_{ox} is the permittivity of silicon dioxide; W is the channel width; L_D is a technological parameter associated with the lateral diffusion of drain below the gate; L is the channel length; t_{ox} is the gate oxide thickness; C'_{ox} is a technological parameter associated with the capacitance per unit area between the gate and the channel.

4.3.2 Pull-in voltage

The next consideration is the pull in voltage, which can be calculated by:

$$V_p = \sqrt{\frac{8}{27}\frac{k_x d^3}{\epsilon_0 A}} \tag{22}$$

As was established before, it is necessary to ensure that none of the input voltages exceed this value; otherwise the risk of driving the plates to a direct contact will be present, causing an undesirable short circuit. This effect is also known as pull-in effect, and is primarily caused by the electrostatic field generated between the two capacitor

Table 1 Parameters for simulation

Variable	Symbol	Proposed value
Movable mass	M	2.5×10^{-10} kg
Applied force due to 6G acceleration	$f(t) = Ma$	G = 6, $f(t) = 147 \times 10^{-10}$ N
Proposed displacement for 6G applied	x	1×10^{-6} m
Stiffness coefficient	$k_x = k$	14.7×10^{-3} N/m
Damping coefficient	b	2.8×10^{-7} Ns/m
Overlapping area	A	7×10^{-9} m^2
Permittivity	$\varepsilon_0\varepsilon_r$	8.85×10^{-12} F/m
Electrode 1 distance	d_1	2×10^{-6} m
Electrode 2 distance	d_2	3×10^{-6} m
Parasitic capacitance	C_D	1.49×10^{-15} F
Parasitic capacitance	C_{OX}	1.8×10^{-14} F
Drain to source voltage	V_{DS}	5 V
Control gate voltage	V_C	5 V

plates forming the sensor, either parallel plate capacitor or a capacitor formed by adjacent plates.

5 Simulation

In order to observe the behavior of the mathematical model, a simulation with the following parameters was performed; the model used for simulation corresponds to Eqs. (4)–(6) (Table 1):

Simulation shows the impulse response of the sensor when $V_{DS} = 5$ V and $V_C = 5$ V was applied to drain and control gate, respectively; a force due to an acceleration of 6G was applied during 5 ms and the response was observed.

Figure 5 shows the displacement of the movable mass for two cases considered: (a) using a conventional model mass–spring–damper; and (b) using the electro-mechanical model, from Eqs. (4)–(6); as it can be seen, the mechanical model shows larger oscillations and longer stabilization time until rest state is reached.

In Fig. 6, the electrical charges of the circuit are shown, something that could not be possible using a purely mechanical model; it can be seen that the waveform of the charge follows the waveform of displacement of the movable mass, as was expected; also it can be observed that charges are not zero at t = 0, since the voltage sources are always connected.

Deriving q_1 in Fig. 6 results in the drain current of the system and it is shown in Fig. 7. This current is very important to be considered in the design of the read out circuitry, since it represents a leakage current. Although the order of magnitude of this current is too low (~10^{-10} A), it is part of the electrostatics affecting the response of the system. Therefore, after the results of this analysis, it can be expected that the larger the swings, the higher the leakage current will be. It should be remembered that q_1 is related with the parasitic coupling capacitance created by the overlap between gate and drain. Due to the lower magnitude of q_2, its contribution will not be considered since, as mentioned before, both terminals of this parasitic capacitance (gate-source overlap) are connected to ground.

This leakage current makes the difference from the pure mechanical model normally used in mass–spring–damper systems. Therefore, the importance of considering the added contribution of electrical elements to the model proposed using a FGMOS as a transducer instead of a pure differential capacitor array is highlighted with these results. It should be remembered that the present analysis was made starting from a given set of proposed values for several parameters, among which the stiffness coefficient is one of them. Nevertheless, the sensor design depends on the acceleration range, the proof mass geometry, etc., giving the

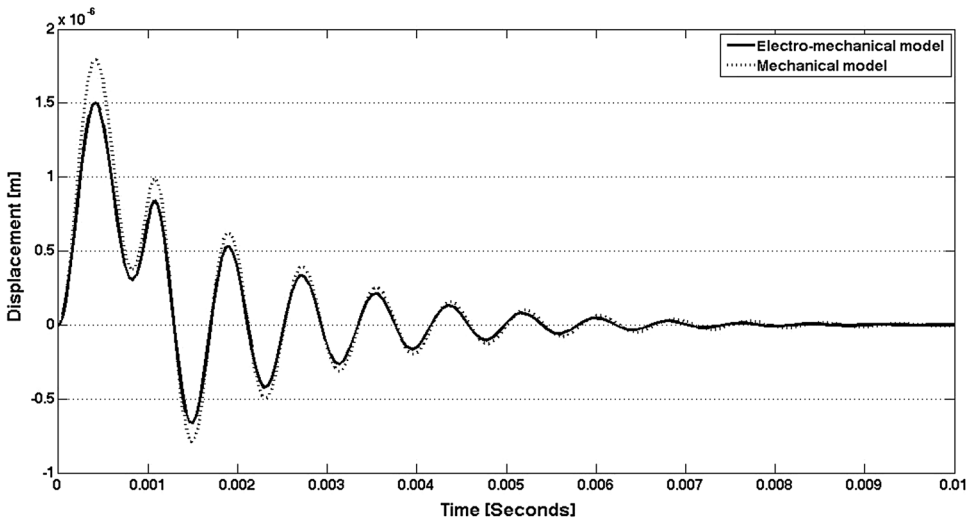

Fig. 5 Impulse response of a capacitive sensor using the model derived in Eqs. (4)–(6)

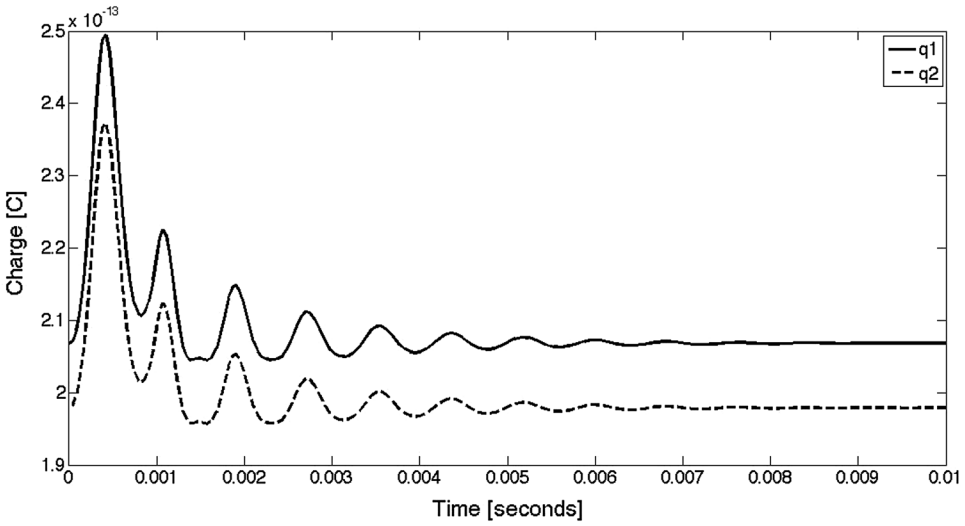

Fig. 6 Charge in the circuit using the model derived in Eqs. (4)–(6)

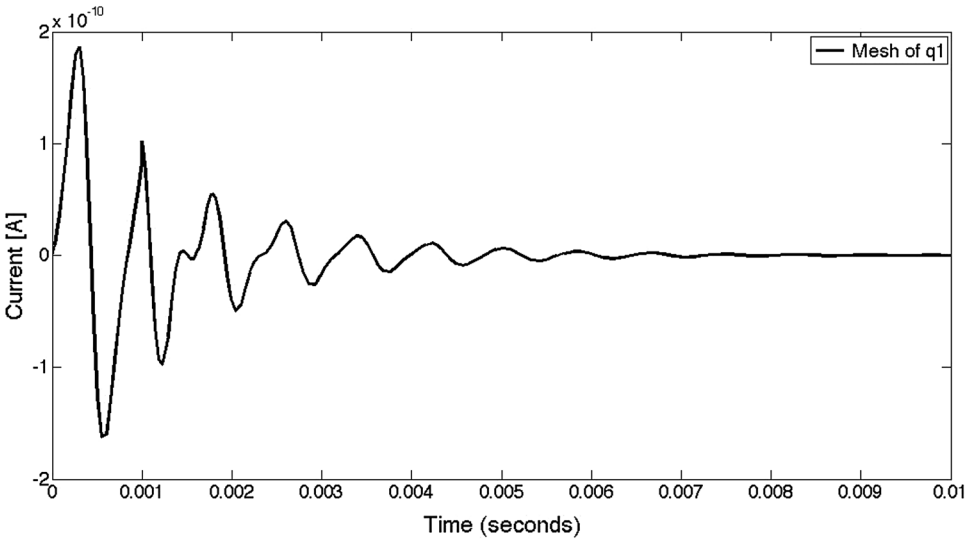

Fig. 7 Drain current in the FGMOS using the model derived in Eqs. (4)–(6)

sensor a wide spread of possible designs but the proposed analysis can be made although for each one.

6 Conclusions

Modeling with Euler–Lagrange proves to be very useful for MEMS development involving a high scale of integration of electronic circuitry, whether it is monolithically integrated or not; this modeling tool is compatible with microsystems and electronic circuitry, allowing considering the energy present in the same physical element and dividing it into different theoretical elements, e.g., systems such as inertial sensors. For instance, it is necessary to consider first a moving mass, then the stiffness associated to it, as well as the damping of the system. Since the CMOS technology from which the sensor is planned to be fabricated is a layered manufacturing process, the MEMS structure must be considered as a whole, realizing that the moving mass, the spring, and the damper also perform as electrical circuit components; this introduces extra complexity to the system modeling. This article shows that the Newton–Euler modeling simplifies modeling micro-systems, and gives a readily and simple alternative from using complex software based on finite elements analysis, which requires heavy software platforms, achieving simplicity and accuracy. Prediction can be easily made with an algorithm which is capable of numerically solving the equations that describe the dynamics of the system.

We also demonstrated that there is a clear difference between getting a purely mechanical model, such as the mass–spring–damper conventional model, compared with a specific electromechanical system, since it is possible to predict the behavior of the system including the effect of

electrical elements and the way they affect the mechanical performance of the microsystem.

Acknowledgments The authors wish to thank CONACyT Project number 124103 and the Micro and Nano Technology Laboratory from the CNMN-IPN for their support.

References

Croci L, Martinez A, Coirault P, Champenois G, Gaubert J-P (2012) Passivity-based control of photovoltaic-wind hybrid system with Euler–Lagrange modeling. 38th Annual Conference on IEEE Industrial Electronics Society (IEEE)

Huei-Huang L (2012) Finite element simulations with ANSYS workbench 14, theory, applications, case studies. SDC

Mezghani B, Tounsi F, Masmoudi M (2013) Sensitivity modeling of dual-axis CMOS MEMS convective accelerometers using FEM and spherical model (©EDA Publishing)

Pustan M, Paquay S, Rochus V, Golinval J-C (2010) Modeling and finite element analysis of mechanical behavior of flexible MEMS components. DTIP (©EDA Publishing)

Su Y, Chong CS (2005) Automatic mixed-dimensional MEMS modeling. International Conference on Advanced Intelligent Mechatronics (IEEE/ASME), pp 24–28

Van Toan N, Ono T (2014) Capacitive silicon resonator structure with movable electrodes to reduce capacitive gap widths based on electrostatic parallel plate actuation. MEMS, San Francisco

Zeng K, Liu Z, Korvink JG (2003) A new methodology for modeling MEMS structures. Design, Test, Integration and Packaging of MEMSiMOEMS (DTIP)

Zeng Z, Yang H, Zhao R, Tang S, Chen LI (2011) An electromechanical coupling model for an inclined drum washing machine vibration system based on Euler–Lagrange theory. International Electric Machines and Drives Conference (IEMDC) (IEEE)

Zhang Z, Liu H (2007) L2-gain control for single-phase active power filter using Euler–Lagrange model. International Symposium on Industrial Electronics, ISIE (IEEE), pp 2469–2474

Zhao C, Wang L, Kazmierski TJ (2007) An efficient and accurate MEMS accelerometer model with sense finger dynamics for applications in mixed-technology control loops. IEEE pp 143–147